

Shape memory alloy mechanical actuator with reduced commutation time

Simón Prêcheur Llarena¹, Loïc Tissot-Daguette¹, Marjan Ghorbani¹, Charles Baur¹, Simon Henein¹

¹École Polytechnique Fédérale de Lausanne, Switzerland

simon.precheur-llarena@epfl.ch

Abstract

Using shape memory alloys (SMAs) as actuators offers several advantages, including high power density, large stroke capabilities, and friction elimination. These attributes make SMAs suitable for actuating flexure-based mechanisms in a wide array of extreme environments. However, their extended cooling time limits their use for applications requiring a high cadence or fast commutation. This paper presents the design of a novel type of mechanical actuator conceived to address this dynamical performance issue. The proposed mechanism is a bistable switch based on a preloaded buckled beam attached to a flexure pivot. The mechanism is actuated by a set of n individual modules, each powered by an SMA spring. Each module is selectively engaged and disengaged from the switch through a selection gear put in motion by a coupling blade. Since only one module is active at any given time, the others can cool down in the meantime: the commutation time is hence reduced by a factor of n compared to a classical antagonistic-pair SMA design. This solution operates passively: it doesn't require active cooling or any additional energy intake.

This innovative and generic design is intended for use with SMA actuated bistable mechanisms, leveraging their advantages to achieve very high accuracy, precision and repeatability while keeping a highly dynamical performance.

Keywords: Design, Mechanism, Actuator, Shape memory alloy

1. Introduction

Shape Memory Alloys (SMA) are a unique class of materials that can recover their original shape when subjected to certain stimuli. By changing the temperature of thermally responsive SMAs, a thermoelastic solid-solid phase transformation occurs. This reversible and diffusionless transformation happens between the high temperature stable phase known as Austenite, and the low-temperature one named Martensite. SMA springs are small, lightweight, and provide large strokes, which makes them well suited for actuation. However, their long cooling time hinders their use in certain applications. Improving the commutation time of SMA-based actuators would provide them with a whole range of new applications in fields where speed is critical, and where volume, total mass, or cost are not as limiting.

Previous published work on this matter includes the exploration of active cooling strategies or periodic heat sink usage [1]. The achieved improvements through these methods are not sufficient and bring additional multifactorial system level complexities. Because of these limitations, a fully mechanical approach was instead researched, resulting in this work.

This paper presents the mechanical concept and characteristics of this new actuator design, followed by an explanation of its kinematics. Then, an analytical model is established and verified by simulations. Finally, two examples of the realization and performance of a metal-based version are presented.

2. Description of the actuator

2.1. Actuation sequence

The commutation time is defined as the time it takes for the end effector of the bistable mechanism to switch from one stable state to the other. Two commutations correspond to a full cycle.

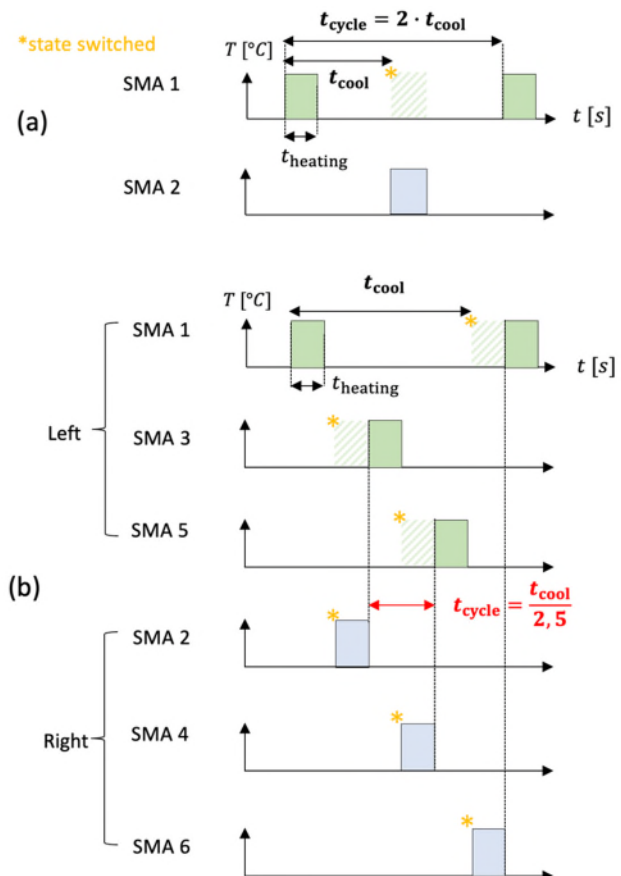


Figure 1. (a) Sequence showing the heating periods (i.e. electrical current delivery) as a function of time in a 2-SMA design. (b) Sequence in a 6-SMA design with the proposed architecture. *Note: The SMAs must be cold and back to the original position when the state switches.

Provided there is no heat convection and good thermal isolation between individual SMA modules, the commutation time t_{commute} is as follows:

$$t_{\text{commute}} = \frac{t_{\text{cycle}}}{2} = \frac{t_{\text{cool}}}{n-1} \quad (1)$$

where t_{cycle} is the time it takes to perform two commutations (the end effector being back to its initial position), t_{cool} is the time one SMA takes to cool down, and n is the number of SMA modules. Since the state of the system is switched every two commutations, the time is divided by $n-1$.

A two SMA system would yield the control sequence in Fig. 1(a). In comparison, selectively decoupling 6 SMAs results in sequence in Fig. 1(b) instead.

The proposed system requires no additional energy input in order to decouple the SMAs during their cooling periods.

2.2. Actuator kinematics

This actuator is a bistable pivoting mechanism with a tunable stroke. The bistability is provided by the use of a buckled beam preloaded by a displacement. It features two stable positions $\pm\theta_{\text{stable}}$ that can be tuned by adjusting a screw.

A minimum of two SMA modules selectively pull on the bistable part to switch from one stable state to the other. When the SMAs are not active, there is an elastic decoupling between them and the end effector, which ensures the actuator still exerts an almost constant force when a displacement is imposed on it [2]. Otherwise, it remains at a stable position. This behavior makes it ideal for the actuation of grippers, for example.

The use of bistability is required to compensate for the SMAs' lack of repeatability in terms of positional inaccuracy [3]. It also makes it possible to run the system without sensors in an open loop (i.e. without sensors). This makes this mechanism well suited for actuating a variety of systems that already operate using bistability, such as the bistable flexure based gripper seen in section 4.2.

The bistable switch acting as the end effector of the actuator (Fig. 2) is at the heart of the system. A beam of length L is preloaded by a displacement Δl . When a critical angle θ_{in} is applied, the buckled beam snaps through and switches state.

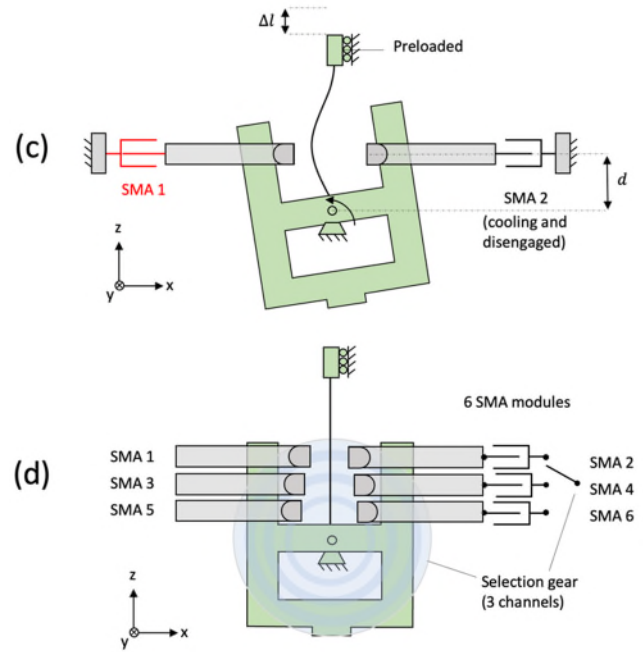
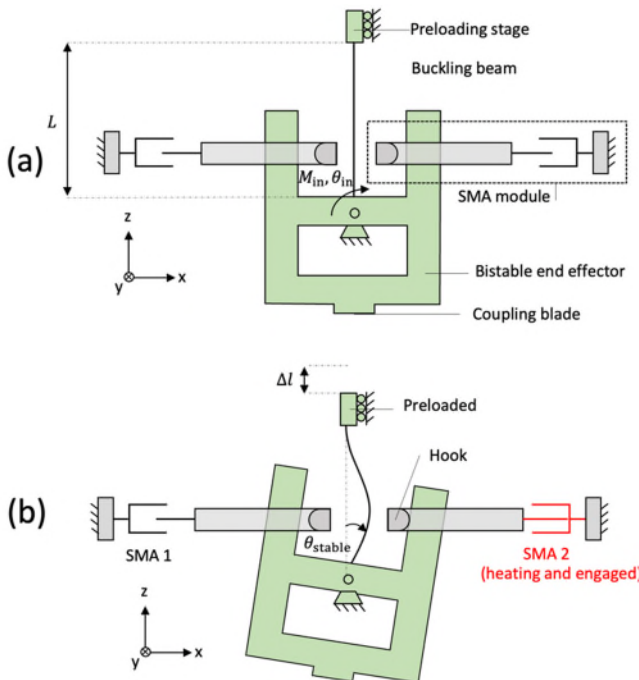


Figure 2. (a) Unloaded bistable stage, (b) Preloaded and actuated on the right, (c) Preloaded and actuated on the left, (d) Version with $n = 6$ stacked modules and selection gear.

An “SMA module” is defined as the subsystem comprised of one SMA spring, a parallelogram linkage spring, and finally a hook mounted on a pivot that actuates the end effector (Fig. 3). The parallelogram linkage guides the SMA in translation and returns it back to its modified open shape as it cools down. Eventually, the SMA is ready to be coupled and heated again, returning to its original size.

The selection gear is a ratchet gear. It is held in place by a pawl on one side of its perimeter (Fig. 3), and driven by the coupling blade on the opposite side. The gear has thus several stable angular positions equal to the number of its teeth, which by construction must be a multiple of $n/2$. The front of the selection gear has one or several circumferential channels where pins shaped like arcs are fixed in a fitting pattern. When superposed with its associated hook, the pin exerts a force against the hook's elastic pivot, engaging it with the end effector. The hook is then ready to be pulled by the SMA. When the latter heats and the SMA pulls, a snap-through occurs and the bistable state of the system is switched. When SMAs on the right pull, the coupling blade pushes against the teeth of the gear, which then rotates until the pawl secures it in the next position. Simultaneously, the pin rotates disengaging the aforementioned hook, decoupling it from the end effector, and allowing it to cool down while the sequence continues. When the SMAs on the left pull, the coupling blade is instead retrograded a notch, the pawl securing the gear in position. As such, the selection gear changes state once every two commutations, in a similar fashion to a clock escapement.

The resistance felt by the coupling blade or pawl blade due to the friction force against the selection gear when changing states should be significantly lower than the force the SMAs exert, for the actuator to be efficient.

All ideal joints are implemented by flexures [4]. The input pivot is embodied by a cross-spring flexure pivot, and parallelogram linkages by parallel leaf-spring stages. The pawl is replaced by an L-shaped blade. The pivot supporting the hook is replaced by a simple blade. The choice of SMA springs is detailed in section 4.

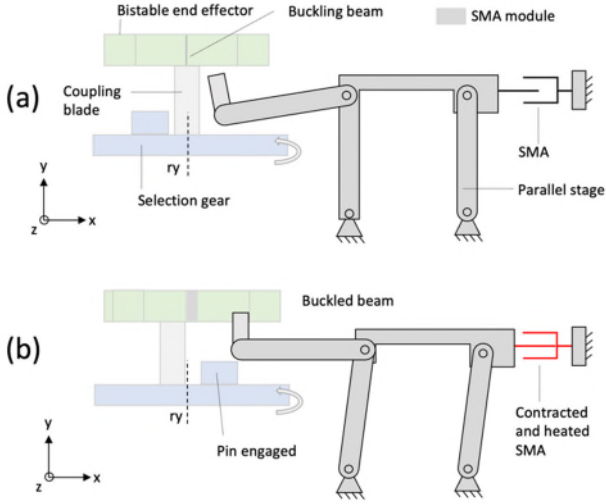


Figure 3. Summarized kinematics of one single SMA module.

2.3. Generalization to multiple SMA modules

When scaling the number of SMA modules up, there is an increase in performance for each additional SMA module at a decreasing marginal cost. Each added SMA module makes the commutation frequency to mass, cost, or volume ratio greater. SMA modules can be added so far as the selection gear's geometrical limitations, and overall volume and mass constraints are met. The theoretical limit to the decrease in commutation time is the time it takes for an SMA to heat and complete a stroke. Therefore, the commutation time will be:

$$t_{\text{heating}} < t_{\text{commute}} = \frac{t_{\text{cool}}}{n-1}, \text{ see Eq. (1)} \quad (2)$$

where t_{heating} is the time required to heat the SMAs to operating temperature.

When scaling up, SMAs must be dimensioned differently according to their actuating distance d from the pivot center of rotation, in order to always achieve the same input torque M_{in} , given by $M_{\text{in}} = d \cdot F_{\text{SMA}}$, where F_{SMA} is the force exerted by the SMA at snap-through angle.

3. Analytical model

An analytical model was established to characterize the behaviour of the mechanism. In a fixed-pinned configuration, the magnitudes of the input angle and torque required to switch the state of a buckled beam are respectively given by [2] as:

$$\theta_{\text{in,lim}} = 1.78 \sqrt{\frac{\Delta l}{L}} \quad (3)$$

$$M_{\text{in,lim}} = 12.90 \frac{EI}{L} \sqrt{\frac{\Delta l}{L}} \quad (4)$$

where EI stands for the flexural rigidity of the buckling beam, L its length, and Δl its shortening. The constants in Eqs. (3) and (4) correspond to limit points in the input moment-angle characteristics of the buckled beam after which snap-through occurs [2]. The whole flexure system resisting the SMA's movement (coupling blade, pawl corner blade, parallel leaf spring stage) shows an equivalent stiffness k_{eq} that acts against the SMA. The linear stroke at which snap-through occurs is [2]:

$$x_{\text{lim}} = d \cdot \sin(\theta_{\text{in,lim}}) \quad (5)$$

Therefore, the condition for snap-through is:

$$F_{\text{SMA}} > \frac{M_{\text{in,lim}}}{d} + x_{\text{lim}} k_{\text{eq}} \quad (6)$$

4. Realisation of the design

By adapting the analytical model to the specifications required, all dimensions were computed for the realization of two CAD versions. The chosen SMA has a Kirigami architecture. It is a novel topology inspired by the Japanese paper cutting and folding kirigami art. It features W shaped cutout patterns which increase the stroke and heat dissipation surfaces, both critical in this use case, in comparison to other conventional alternatives such as wires [3]. The material used is NiTiNOL.

4.1. 2-SMA metal prototype

A version using the full kinematics and only 2 SMA modules is proposed (Fig. 4). Its fabrication is intended with the goal of testing the kinematics, and the adequacy of the measurements with the analytical model, without creating a full stack version. The proposed dimensions are: thickness of the buckled beam: 150 μm , thickness of cross spring blades: 100 μm , angle of actuation, $\theta_{\text{stable}} = 12^\circ$, $F_{\text{SMA}} = 3 \text{ N}$, and a stroke of 4 mm.

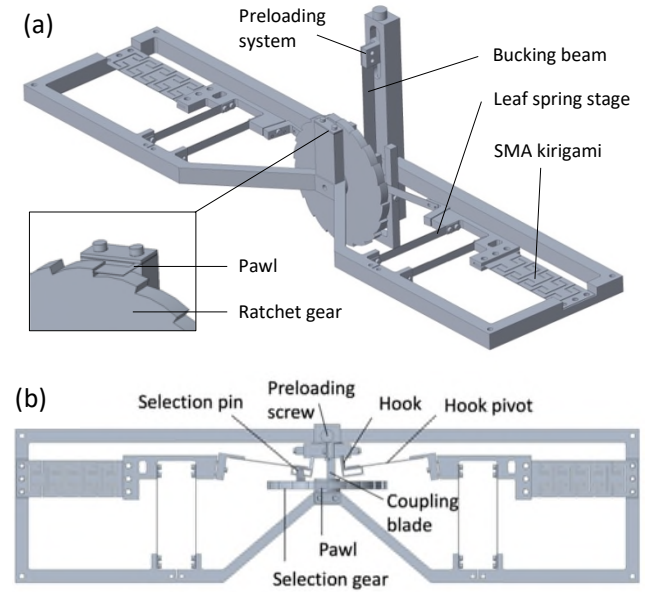


Figure 4. 2 CAD views of a metal 2-SMA prototype. The pawl is shown in the bottom left corner. SMAs are not displayed at the nominal position.

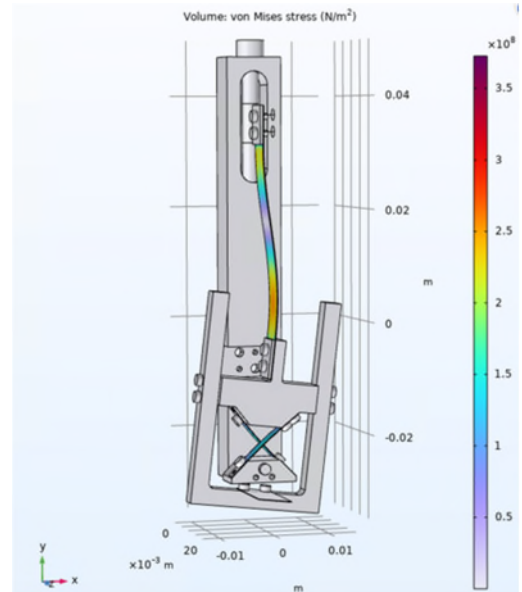


Figure 5. FEM simulations showing von Mises stress for the buckling beam and cross pivot, as well as the end effector in a stable state.

FEM simulations were conducted to validate the design and ensure that stress limits were not surpassed. Fig. 5 shows that stress does not exceed the steel's yield strength at maximum stroke.

4.2. Metal prototype for flexure-based gripper actuation

Fig. 6 shows a concrete use case, where the system was implemented on a bistable gripper flexure based mechanism [5]. This particular design uses 3 SMA modules on each of 4 quadrants, thus a total of $n = 12$ SMAs. The wheel has $n/n_{\text{quadrant}} = 3$ channels. Using properly dimensioned SMAs with $t_{\text{cool}} = 4$ s, we have $t_{\text{commute}} = \frac{t_{\text{cool}}}{11} = 364$ ms.

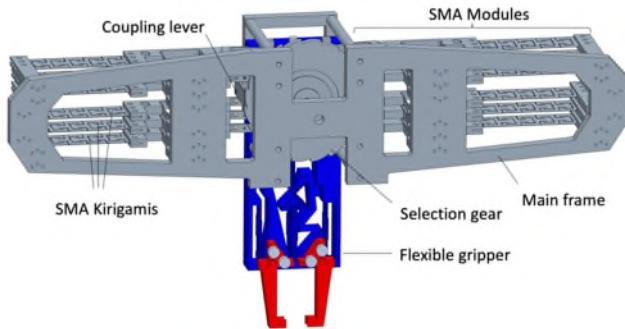


Figure 6. CAD view of a metal 12-SMA prototype mounted on a gripper.

5. Discussion

5.1. Optimization and limits to this design

While lowering the virtual cooling time of SMAs in a fully mechanical way, this approach comes at the expense of volume, mass, and cost. Optimizing the design for reducing these parameters is possible and should be sought in further developments, which are outside the scope of this article. The selected manufacturing process will be critical. Opting for an electro-eroded monolithic design for each module may reduce the costs in comparison to traditional manufacturing techniques requiring assembly. It also requires fewer parts which will reduce mass. Topology optimization can further help in that regard. The choice of materials will also impact mass. Although dense, metal offers great thermal dissipation which is essential to lower SMA cooling times. A proper characterization of the thermal performance will aid in choosing a proper material.

The stacking of SMA sheets might impact the thermal dissipation and thus affect the cooling time of the actuator. The actuation sequence heats the SMAs that are furthest from each other sequentially, which minimizes this effect. Notwithstanding, this effect should be properly estimated and to further mitigate the effect, a thermal insulation layer should be added between the modules, in a material such as a polymer.

5.2. Control and sensors

A current supply and a microcontroller control the n relays that drive the SMA modules, to ensure the right sequence is applied. Current heats the SMA through Joules Effect. It should be noted that the SMA modules should be electrically insulated from the frame to avoid short circuits.

In stable conditions, and given the bistable nature of this actuator, it can safely be used in an open loop, without sensors or encoders. However, proximity sensors can be used to check whether the switches were correctly realised. This would be useful in perturbed environments, to ensure that temperature or humidity do not tamper performance. Furthermore, such a sensor would be useful to run an automatic calibration routine, or to optimize performance dynamically during use.

Finally, it is possible to motorize the screw preloading the buckled beam, so that the stroke and exerted force can be tuned dynamically. In the case of the gripper section 4.2, such a setting would be useful to dynamically adjust the strength of the prehension, modulating the kind of weight that can be carried.

5.3. Dynamical behaviour

Due to the significant mass of the metal moving parts, external acceleration and gravity cannot be neglected. Dynamically balancing the SMA modules would fix that, but at the cost of extra mass and volume. To compensate for gravity without adding mass, both prototypes in section 4 feature horizontal SMA modules. Using a vertical design instead would induce a gravitational force on the SMA equivalent to $P \approx 0.4 \cdot F_{SMA}$. To keep the compensation, the actuator must be mounted on a tool operating with 4 degrees of freedom (three translational and one rotational: x, y, z, r_z). The mechanism would work in all orientations (6 degrees of freedom) if the modules were resized so that the SMAs can exert more force to accommodate gravity. This would rack up some extra mass, volume, and cost.

6. Conclusion

The mechanical concept and the actuator's working principle were described. An analytical model and its associated simulations were presented. Finally, examples for the realization of two metal-based versions were shown.

The potential for mechanical actuators coupling and decoupling several individual actuators was established. This innovative concept is promising in the context of Shape Memory Alloys in order to increase significantly the actuation rate.

Future work includes testing and realizing measurement campaigns on the prototype following its fabrication. Namely, the experimental validation of the analytical model and eventually the development of the device into a more optimized version, with a set of specifications. These elements together will help determine the usability of this system in industrial applications. If successful, this type of device could expand the range of SMA applications to cases where high cadence, performance and repeatability are required, whilst leveraging their compatibility to environments such as clean rooms, vacuums, space, or contamination-free biological applications [6, 7].

References

- [1] Lara-Quintanilla A, Bersee H E N 2015 Active Cooling and Strain-Ratios to Increase the Actuation Frequency of SMA Wires *J. Shap. Mem. Superelasticity* **1** 460–467
- [2] Tissot-Daguette L, Schneegans H, Thalmann E, Henein S 2022 Analytical modeling and experimental validation of rotationally actuated pinned–pinned and fixed–pinned buckled beam bistable mechanisms *J. Mechanism and Machine Theory* **174** 104874
- [3] Ghorbani M, Thomas S, Lang G, Martinez T, and Perriard Y 2023 Fabrication and Characterization of the Kirigami-Inspired SMA-Powered Actuator *IEEE Transactions on Industry Applications*, **59**
- [4] Cosandier F, Henein S, Richard M, Rubbert L 2017 *The art of flexure mechanism design* EPFL Press Lausanne
- [5] Tissot-Daguette L, Prêcheur Larena S, Baur C and Henein S 2024 Fully compliant snap-through bistable gripper mechanism based on a pinned-pinned buckled beam *24th Euspen conference*
- [6] Zanaty M, Fussinger, T, Rogg A, Lovera A, Lamberlet D, Vardi I, Wolfensberger T J, Baur C, and Henein S 2019 Programmable Multistable Mechanisms for Safe Surgical Puncturing *ASME. J. Med. Devices* **13(2)** 021002
- [7] Power M, Barbot A, Seichepine F and Yang G 2023, Bistable, Pneumatically Actuated Microgripper Fabricated Using Two-Photon Polymerization and Oxygen Plasma Etching *J. Adv. Intell. Syst.*, **5** 2200121